

New search strategy for high z intervening absorbers: GRB 021004, a pilot study^{*}

P. M. Vreeswijk¹, P. Møller², and J. P. U. Fynbo^{3,4}

¹ European Southern Observatory, Alonso de Cordova 3107, Casilla 19001, Santiago 19, Chile

² European Southern Observatory, Karl-Schwarzschild-Strasse 2, D-85748, Garching bei München, Germany

³ Department of Physics and Astronomy, Århus University, Ny Munkegade, DK-8000 Århus C, Denmark

⁴ Astronomical Observatory, Copenhagen University, Juliane Mariesvej 30, DK-2100 København K, Denmark

Received 14 May 2003 / Accepted 6 August 2003

Abstract. We present near-infrared narrow- and broad-band imaging of the field of GRB 021004, performed with ISAAC on the UT1 of the ESO *Very Large Telescope*. The narrow-band filters were chosen to match prominent emission lines at the redshift of the absorption-line systems found against the early-time afterglow of GRB 021004: [O III] at $z=1.38$ and H α at $z=1.60$, respectively. For the $z=1.38$ system we find an emission-line source at an impact parameter of $16''$, which is somewhat larger than the typical impact parameters of a sample of Mg II absorbers at redshifts around unity. Assuming that this tentative redshift-identification is correct, the star formation rate of the galaxy is $13\pm 2 M_{\odot} \text{ yr}^{-1}$. Our study reaches star-formation rate limits (5σ) of $5.7 M_{\odot} \text{ yr}^{-1}$ at $z=1.38$, and $7.7 M_{\odot} \text{ yr}^{-1}$ at $z=1.60$. These limits correspond to a depth of roughly $0.13 L^*$. Any galaxy counterpart of the absorbers nearer to the line of sight either has to be fainter than this limit or not be an emission-line source.

Key words. gamma rays: bursts – galaxies: distances and redshifts – quasars: absorption lines

1. Introduction

Identification of the objects responsible for the high redshift intervening absorption systems in QSO spectra, such as Damped Ly α (DLA) and Mg II absorbers, has been the expressed goal of a large number of observing programmes over the past 2 decades (e.g. Smith et al. 1989; Deharveng et al. 1990; Le Brun et al. 1997; Guillemin & Bergeron 1997; Warren et al. 2001; Kulkarni et al. 2001; Colbert & Malkan 2002). Even though many such programmes have been successful in detecting objects at (or near) the absorption redshift, a doubt does in almost all cases persist as to whether the identified object is indeed the absorber or if there could be another object hidden inside the glare of the QSO itself at much smaller impact parameter. It was only realized very late that this problem is seriously exacerbated by the strong bias of the absorption cross-section selection which picks out mostly objects with the smallest impact parameters (Fynbo et al. 1999; Schaye 2001; Møller et al. 2002b). The discovery of bright, high-redshift optical transients (OTs) of gamma-ray bursts (GRBs) has now made it possible to completely eliminate this last doubt. GRB

OTs, like QSOs, allow identification of high-redshift absorbers, but the OTs, unlike QSOs, fade away completely within a few months leaving the spectroscopically investigated sightline open for extremely deep imaging studies.

The current status concerning the galaxy counterparts is the following. For the high- z ($z>2$) DLA sample, the debate has been between advocates for large, disk-forming galaxies (Wolfe et al. 1986; Prochaska & Wolfe 2001) and faint and small, gas-rich dwarfs (Tyson 1988; Haehnelt et al. 1998). In three cases DLA absorbing galaxies have been identified as faint blue Ly α emitting galaxies at impact parameters ranging from 0.99 to 2.51 arcsecs (8–19 kpc), supporting the view that DLA galaxies at $z>2$ are faint blue dwarf galaxies (Møller et al. 2002b). In the range from $z=0$ to $z=1.2$, Guillemin & Bergeron (1997) reported that galaxy counterparts of Mg II absorbers with equivalent widths larger than 0.6 \AA predominantly are spirals with luminosities similar to present-day L^* galaxies. The impact parameters of the identified galaxies were found to correlate with the luminosities of the galaxies, such that bright galaxies are found at larger impact parameters. In a flux limited study, objects below the given detection limit will fail to be identified, and because of the correlation with impact parameter this will tend to bias all identifications both towards brighter objects and towards larger impact parameters. An indication that this

Send offprint requests to: pvreeswi@eso.org

^{*} Based on observations collected at the European Southern Observatory, Chile; proposal no. 270.A-5016

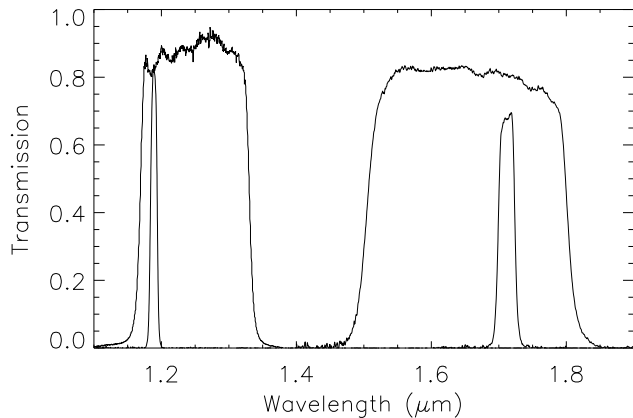


Fig. 1. The transmission curves for the four filters used in this project. From left to right it is Js, NB 1.19, H, NB 1.71.

may be the case for the MgII studies is the clear tendency for higher redshift absorbers to be identified as brighter galaxies with larger impact parameters (around 110 kpc at $z=1.1$) than those at lower redshifts (around 20 kpc at $z=0.1$). The actual absorbers may therefore still be hiding at small impact parameters below the detection limit.

GRB 021004 is the third brightest afterglow detected so far, with $R=15.4$ only 4 minutes after the burst (Fox et al. 2003). Spectroscopic observations (e.g. Chornock & Filippenko 2002) found a host galaxy redshift of $z=2.33$. In addition two other systems were identified with absorption lines of MgI, MgII (both systems with equivalent widths larger than 0.6 \AA), and Fe II at $z=1.38$ and $z=1.60$ (e.g. Møller et al. 2002a). In this pilot study we present observations in narrow- and broad-band filters to search for emission lines from the galaxy counterparts of these absorbers. The emission-line imaging technique that we employ allows identification of the foreground absorber, even when it would be located exactly along the line of sight to the GRB and its host galaxy. Throughout the paper we assume $H_0 = 70 \text{ km s}^{-1} \text{ Mpc}^{-1}$, $\Omega_m = 0.3$ and $\Omega_\lambda = 0.7$.

2. Observations

At $z=1.38$, [O III] $\lambda 5007$ is redshifted to 1.19 \mu m , and at $z=1.60$, H α emission is shifted to 1.71 \mu m . These wavelengths correspond to the central wavelengths of two ISAAC narrow-band filters. Imaging in these two filters and in the Js and H band allows identification of the intervening systems if they are star-forming galaxies. In Fig. 1 we show the filter transmission curves for the four filters.

The observations were carried out in service mode with UT1/ISAAC of ESO's *Very Large Telescope* on the nights of December 17/18 and 19/20, 2002, for a total effective exposure time of 51 and 105 minutes in the narrow-band filters NB 1.19 and NB 1.71, respectively. To enable continuum subtraction, we also observed the field in the broad-band filters Js and H, each for 11 minutes. Table 1 shows the log of the observations. The ISAAC short-

Table 1. Log of observations

filter	obs.date 2002 UT	DIT (sec)	NDIT	NINT	exp.time (sec)	seeing ($''$)
NB1.71	Dec 18.062	50	3	42	6300	0.53
NB1.19	Dec 20.055	60	3	17	3060	0.70
H	Dec 20.086	10	6	11	660	0.60
Js	Dec 20.098	30	2	11	660	0.56

wavelength detector is a Rockwell 1024x1024 chip, with a gain of 4.5 electrons/ADU, a read noise of 11 electrons and a pixel-size of $0''.148$.

From the raw images possible ghosts of especially bright objects were removed with the *ECLIPSE* (Devillard 2001) routine *ghost*. After dark subtraction, the flat-field for each image was constructed using the *ECLIPSE* routine *tuflat*. After flat-fielding and removal of bad pixels using the *fixpix* task within *IRAF*¹, the sky was determined for each image from the adjacent images on either side. In the case of the narrow-band filters, we used four images on either side, and for the broad-band filters we used as many as possible (10). We performed two sky passes. In the first pass all object images of a particular Observation Block (OB) are sky subtracted. These images are registered with a shift only (i.e. no scaling nor rotation) to the coordinate system of the first image of the OB using about 5 bright objects in the field, and combined. From this image we make an object mask using the optional output image from *SExtractor* (Bertin & Arnouts 1996), which returns the pixels above the noise of the detected objects. With *imreplace* in *IRAF*, these objects were transformed into a bad pixel mask, making them larger by a few pixels. Then we perform another sky run, this time with all objects masked while average-combining the adjacent sky images. Again we register the images, and now combine them using the *sigclip* rejection in *imcombine* within *IRAF*, which excludes possible cosmic rays and bad pixels that were missed. Finally, residuals left from bias variations and possible horizontal jumps were removed by subtracting the median of each row and/or column of the image using *ECLIPSE* routines. This median was determined from the final image with the objects masked. The final reduced images were trimmed to a size of $2'$ by $2'$, which is the part of the image that was exposed in each sub-exposure (the size of the original images is $2'.5$ by $2'.5$, while we set the jitter box width to $30''$).

We used observations of the NICMOS standard 9123 (S427-D) (Persson et al. 1998) to calibrate the narrow bands and observations of the UKIRT faint standards FS6 and FS32 (Hawarden et al. 2001) to calibrate the Js and H bands. For the broad bands, no correction for a colour

¹ IRAF is distributed by the National Optical Astronomy Observatories, which are operated by the Association of Universities for Research in Astronomy, Inc., under cooperative agreement with the National Science Foundation.

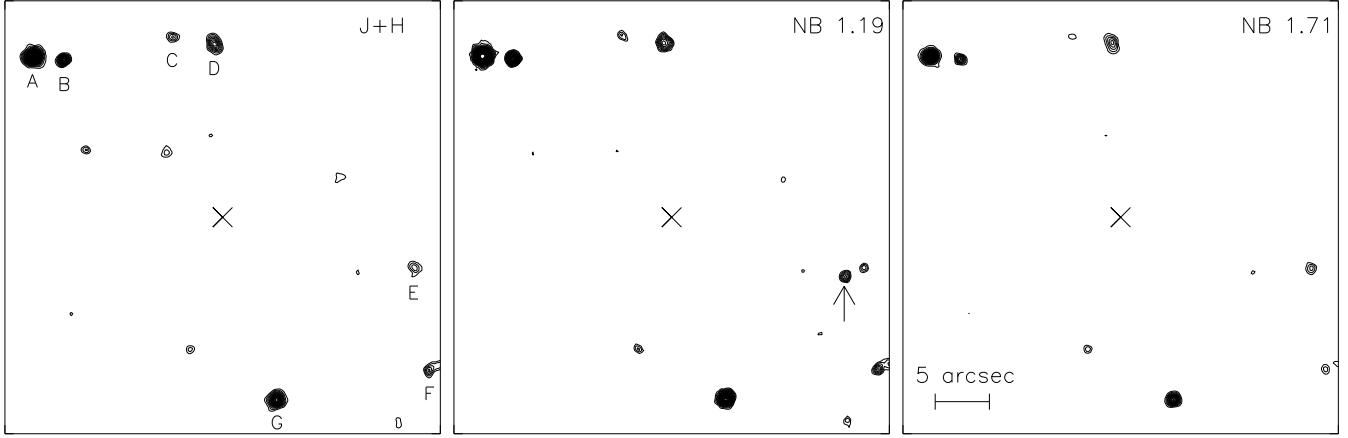


Fig. 2. A 40×40 arcsec² field centred on the position of GRB021004 from the sum of the Js and H band images (left), the NB 1.19 image (middle), and the NB 1.71 images (right). The only emission-line source closer in than $30''$ is a candidate [O III] emitter at an impact parameter of $16''$ seen near the western edge of the NB 1.19 image.

term was attempted. We corrected for atmospheric extinction assuming an extinction of 0.06 mag per unit airmass. We estimate that the uncertainties on the zero-points are 0.04 and 0.10 for Js and H respectively. The zeropoints for the narrow-band filters are determined by integrating the spectrum of S427-D over the filter transmission curves to obtain the flux in $\text{erg s}^{-1} \text{cm}^{-1}$ outside the atmosphere.

3. Emission-line candidates

Inspection of the images reveals no emission in any of the filters at the location of the early-time afterglow of GRB021004. To select emission-line candidates we follow a method similar to the one outlined in Fynbo et al. (1999). We let *SExtractor* (Bertin & Arnouts 1996) detect objects using a very low threshold, i.e. requiring that 2 adjacent pixels are at least 1.5 sigma above the sky. For all detected sources we perform aperture photometry with the *phot* routine in *IRAF*, after which we reject all objects with a signal-to-noise ratio less than 5. The aperture is set to a radius of 6 pixels ($0''.9$ on the sky) for all images. This roughly corresponds to 1.5 times the size of the full width at half maximum (FWHM) of the average image point-spread function (PSF). The local sky was determined in an annulus 10 pixels wide, at a distance of 10 times the image FWHM (about 40 pixels) from the object centre. The coordinates of the objects found on the narrow-band images were transformed to the broad-band images, and at these locations aperture photometry was performed in exactly the same manner, irrespective of an object being present or not.

In both narrow-band images we detect a number of emission-line candidates (6 in NB 1.19 and 4 in NB 1.71 above 5σ), but almost all at very large impact parameters ($>30''$). Only one candidate in the NB 1.19 image, i.e. [O III] at $z=1.38$, has a small enough impact parameter to be a possible galaxy counterpart of the absorber consistent with the sample identified by Guillemin & Bergeron (1997). It is located at $16''$ from the GRB line-of-sight and

can be seen at the western edge of the section of the field shown in Fig. 2. In Fig. 3 we show the spectral energy distributions of the seven continuum objects named A–F in Fig. 2 and of the [O III] emission-line candidate named O IIIa. Although the emission-line nature of this object is clear, follow-up spectroscopy is needed to verify the redshift.

The NB 1.19 emission-line flux of O IIIa is $8.1 \times 10^{-17} \text{ erg s}^{-1} \text{cm}^{-2}$, while its continuum 3σ upper limit, estimated from the Js and H upper limits, is $2.1 \times 10^{-17} \text{ erg s}^{-1} \text{cm}^{-2}$ in the NB1.19 filter. Under the assumption that the emission line is indeed [O III], the candidate is at a luminosity distance of $3.0 \times 10^{28} \text{ cm}$ and has an [O III] luminosity of $L_{[\text{O III}]} = 7 \times 10^{41} \text{ erg s}^{-1}$. Using the empirical flux ratio [O III]/ $H\alpha$ of 1/2 (based on Table 5 of Guillemin & Bergeron (1997)), we obtain an estimated $H\alpha$ luminosity of $1.4 \times 10^{42} \text{ erg s}^{-1}$. This corresponds to a star-formation rate (SFR) of $13 \pm 2 M_{\odot} \text{ yr}^{-1}$ (Kennicutt 1998). The error given here is the measurement error; an additional error of order 30% originates from the uncertainty in the $H\alpha$ luminosity to SFR conversion factor (Kennicutt 1998).

Our observations are sensitive to a limiting luminosity (5σ with an aperture radius of 6 pixels, and assuming the continuum contribution in the narrow-band filters is negligible compared to the emission line) of $L_{[\text{O III}]} = 3.6 \times 10^{41} \text{ erg s}^{-1}$ at $z=1.38$, and $L_{H\alpha} = 9.7 \times 10^{41} \text{ erg s}^{-1}$ at $z=1.60$. The $H\alpha$ luminosity is about $0.13 L^*$ relative to the Schechter parametrisation of the $H\alpha$ luminosity function of galaxies at similar redshifts of Yan et al. (1999). These luminosity limits correspond to star-formation rates of $\text{SFR}_{z=1.38} = 5.7 M_{\odot} \text{ yr}^{-1}$ and $\text{SFR}_{z=1.60} = 7.7 M_{\odot} \text{ yr}^{-1}$ (Kennicutt 1998).

4. Discussion

The $16''$ impact parameter of the NB 1.19 candidate corresponds to 135 kpc at $z=1.38$. The sample of quasar absorption-line systems identified with galaxies by

Guillemin & Bergeron (1997) were found to have separations of 1.9–23'' which, in the cosmology that we assume, correspond to 12–127 kpc. Our candidate is therefore consistent with, but in the upper range of, the impact parameters of the Mg II systems previously studied. However, we find 9 emission-line objects down to a limiting SFR of $7.7 M_{\odot} \text{ yr}^{-1}$ in two fields each of angular size $2' \times 2'$, so there is a priori 50% chance that one of those objects would be found within an impact parameter of 16'' in one of the fields.

In conclusion, this pilot study is consistent with the result of Guillemin & Bergeron (1997) that the typical Mg II absorber is an L^* galaxy at an impact parameter of 100 kpc. In our case the candidate absorber is less luminous, but in the upper end of the impact parameter distribution. In their intermediate redshift (0.7–1.2) sample, Guillemin & Bergeron identified 10 of 16 absorbers but failed to find counterparts to the remaining 6. We find one but fail to identify a candidate in the other field, while our star-formation limit (see above) compared to theirs ($\text{SFR}_{z=0.7-1.3}=0.7-43 M_{\odot} \text{ yr}^{-1}$) is such that we would have expected to detect half of the objects they identified.

The question therefore remains open whether these large galaxies are really the absorbers, or if they are merely the brightest neighbour to dwarf galaxy absorbers. For DLA absorbing galaxies at higher redshifts impact parameters are found to be of order 10 kpc rather than 100

kpc (Møller et al. 2002b), and the SFRs of order $5-7 M_{\odot} \text{ yr}^{-1}$. This is just below the 5σ limit of our current data. A future larger study of GRB intervening Mg II and DLA absorbers should aim at reaching at least a factor of three deeper (in SFR) in order to answer the question if we are still missing a population of faint absorbers at low impact parameters, and if Mg II absorbers are in fact related to dwarf galaxies of the DLA type.

Acknowledgements. We are grateful to the ESO staff in Garching and Paranal, in particular to Mario van den Ancker and Rachel Johnson, for allowing prompt execution of our proposal. PMV is also thankful to John Willis, Chris Lidman and Sara Ellison for very helpful discussions. JPUF gratefully acknowledges support from the Carlsberg Foundation.

References

- Bertin, E. & Arnouts, S. 1996, *A&AS*, 117, 393
 Chornock, R. & Filippenko, A. V. 2002, *GRB Circular Network*, 1605
 Colbert, J. W. & Malkan, M. A. 2002, *ApJ*, 566, 51
 Deharveng, J. M., Bowyer, S., & Buat, V. 1990, *A&A*, 236, 351
 Devillard, N. 2001, in *ASP Conf. Ser. 238: Astronomical Data Analysis Software and Systems X*, Vol. 10, 525
 Fox, D. W., Yost, S., Kulkarni, S. R., et al. 2003, *Nature*, 422, 284
 Fynbo, J. U., Møller, P., & Warren, S. J. 1999, *MNRAS*, 305, 849
 Guillemin, P. & Bergeron, J. 1997, *A&A*, 328, 499
 Haehnelt, M. G., Steinmetz, M., & Rauch, M. 1998, *ApJ*, 495, 647
 Hawarden, T. G., Leggett, S. K., Letawsky, M. B., Ballantyne, D. R., & Casali, M. M. 2001, *MNRAS*, 325, 563
 Kennicutt, R. C. 1998, *ARA&A*, 36, 189
 Kulkarni, V. P., Hill, J. M., Schneider, G., et al. 2001, *ApJ*, 551, 37
 Le Brun, V., Bergeron, J., Boissé, P., & Deharveng, J. M. 1997, *A&A*, 321, 733
 Møller, P., Fynbo, J. P. U., Hjorth, J., et al. 2002a, *A&A*, 396, L21
 Møller, P., Warren, S. J., Fall, S. M., Fynbo, J. U., & Jakobsen, P. 2002b, *ApJ*, 574, 51
 Persson, S. E., Murphy, D. C., Krzeminski, W., Roth, M., & Rieke, M. J. 1998, *AJ*, 116, 2475
 Prochaska, J. X. & Wolfe, A. M. 2001, *ApJ*, 560, L33
 Schaye, J. 2001, *ApJ*, 559, L1
 Smith, H. E., Cohen, R. D., Burns, J. E., Moore, D. J., & Uchida, B. A. 1989, *ApJ*, 347, 87
 Tyson, N. D. 1988, *ApJ*, 329, L57
 Warren, S. J., Møller, P., Fall, S. M., & Jakobsen, P. 2001, *MNRAS*, 326, 759
 Wolfe, A. M., Turnshek, D. A., Smith, H. E., & Cohen, R. D. 1986, *ApJS*, 61, 249
 Yan, L., McCarthy, P. J., Freudling, W., et al. 1999, *ApJ*, 519, L47

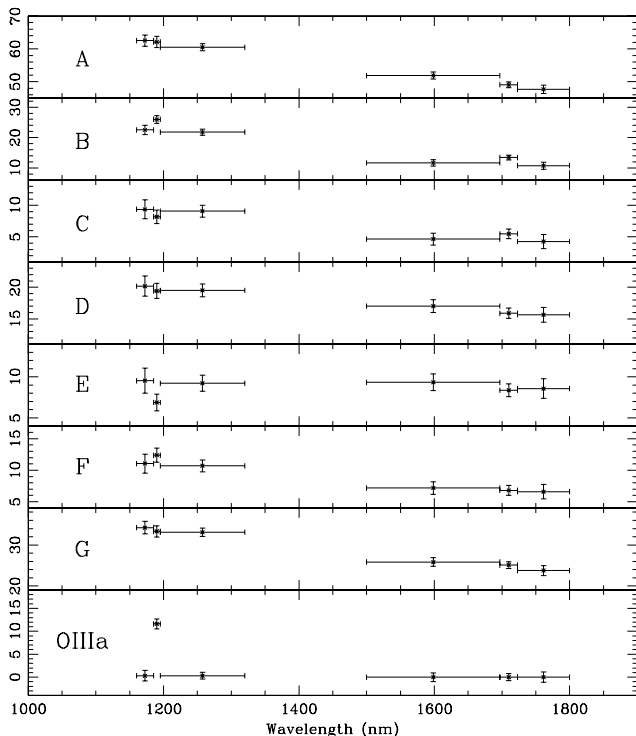


Fig. 3. Spectral energy distributions (proportional to F_{λ}) of the seven objects A–F marked in Fig. 2 and for the candidate $z=1.38$ [O III] emitter. The candidate, named O IIIa and shown at the bottom, has strong excess flux in the NB 1.19 filter.